Test and analysis of MR mounting system for automotive engines

Bai, Guo-Dong, Liu, Qing, Bai, Xian-Xu, Liu, Zhi-Hao, Du, Hao

Guo-Dong Bai, Qing Liu, Xian-Xu Bai, Zhi-Hao Liu, Hao Du, "Test and analysis of MR mounting system for automotive engines," Proc. SPIE 11376, Active and Passive Smart Structures and Integrated Systems IX, 1137610 (22 April 2020); doi: 10.1117/12.2556144

SPIE.

Event: SPIE Smart Structures + Nondestructive Evaluation, 2020, Online Only, California, United States

Test and analysis of MR mounting system for automotive engines

Guo-Dong Bai[1], Qing Liu[1,2], Xian-Xu 'Frank' Bai[1*], Zhi-Hao Liu[3] and Hao Du[1]
[1] Laboratory for Adaptive Structures and Intelligent Systems (LASIS), Department of Vehicle Engineering, Hefei University of Technology, Hefei 230009, People's Republic of China
[2] Tai'an Special Vehicle Co., Ltd, Tai'an 271000, People's Republic of China
[3] Xi'an Research Institute of High Technology, Xi'an 710025, People's Republic of China

ABSTRACT

Vibration of the automotive engine has the characteristics of wide frequency band, multi-vibration sources and multi-main frequencies. Limited capability of passive mounting systems can be provided for engine vibration isolation. A MR semi-active mounting system for automotive engines is investigated in this paper. The dynamic model of the vertical vibration isolation system for the engine and an efficient damping control model of the MR mount are established. The frequency characteristics of the engine vibration are analyzed. The fuzzy control algorithm for the MR mounting system is designed, and the isolation performance of the MR mounting system is analyzed based on the developed experimental setup in Hefei University of Technology.

Keywords: Magnetorheological (MR) fluids; MR mount; engine; vibration isolation; frequency identification

1. INTRODUCTION

Magnetorheological (MR) mounts with different structures and performances have been applied in various vibration control systems [1-6] and have been a hot research topic that has attracted worldwide attentions. Choi's group proposed a shear-flow hybrid mode MR mount [7]. Nondimensional model of the MR mount based on the constitutive equations was developed, and further the nondimensional parameters of the model was analyzed for the MR mount design. To meet the requirement of large controllable damping force in diesel engine mount system, Choi's group further proposed and studied a MR mount with an annular-disc duct [8]. An indirect fuzzy-sliding mode controller was designed to suppress the unwanted vibration. As for the automotive engine mount systems, we investigated a novel unidirectional MR squeeze mount fulfilled with only 22 ml MR fluids [9,10].

However, the existing MR mounts with damping holes or inertia channel would be blocked when under high-frequency excitations. Although the decouplers are employed, fluidic resonance will still increase the field-off dynamic stiffness of the conventional MR mounts. At the same time, the controllability of the damping force is limited due to the block of the damping hole or inertia channel. In addition, the conventional MR mounts require a large amount of MR fluids because of the large fluid chamber, which will increase the cost. We tried to design a MR mount in squeeze mode, but the controllability is limited due to the squeeze gap. The application of the squeeze MR mounts therefore is limited [9,10].

To solve the issue of the existing techniques and maximize the controllability of MR mounts for engine, a new structure of MR mount with an internal bypass (MRM-IB) is proposed. It features a large dynamic stiffness range, small field-off dynamic stiffness and long working stroke. The model of the MRM-IB is established. A fuzzy controller is designed for the MR mounting system according to the vibration characteristics of engines.

2. MRM-IB MOUNT STRUCTURE

Figure 1 shows the principle of the proposed MRM-IB. As shown in Figure 1, the proposed MRM-IB is composed of a main rubber spring unit and a MR damping unit. The main rubber spring unit is set outside of the MR fluid chamber to support static loads. The MR damping unit is composed of a piston assembly, a MR fluid chamber and an annular MR fluid channel sandwiched by two concentric cylinders (i.e., the inner and outer cylinders). Axial motion of the piston assembly along the inner cylinder leads to the flow of MR fluids inside the annular MR fluid channel and inner cylinder, which induces the parallel action of the piston assembly and MR damping unit. So that, MR fluids in the annular channel

* Corresponding author: bai@hfut.edu.cn (Xian-Xu 'Frank' Bai); http://www.lasiser.com

Active and Passive Smart Structures and Integrated Systems IX, edited by Jae-Hung Han, Gang Wang, Shima Shahab,
Proc. of SPIE Vol. 11376, 1137610 · © 2020 SPIE · CCC code: 0277-786X/20/$21 · doi: 10.1117/12.2556144

work in pure flow mode. Continuous controllable damping/stiffness can be realized by adjusting the applied current in the electromagnetic coil winding, which are wound around the annular groove of the inner cylinder.

Damping force F of the MRM-IB is:

$$F = \Delta P \cdot A_{\mathrm{p}} \tag{1}$$

$$\Delta P = \Delta P_{\tau} + \Delta P_{\eta} + \Delta P_{\mathrm{I}} \tag{2}$$

where ΔP_{τ} is the pressure drop due to the MR effect; ΔP_{η} is the pressure drop due to the viscosity effect; ΔP_{I} is the pressure drop due to the inertia effect; A_{p} represents the effective area of the piston. The pressure drop due to the MR effect is:

$$\Delta P_{\tau} = \frac{2L\tau_{\mathrm{y}}}{\Delta R}\mathrm{sgn}(\dot{x}_{\mathrm{r}}) \tag{3}$$

where L and ΔR respectively represent the length and width of the MR fluid channel; $\dot{x}_{\mathrm{r}}$ is the flow velocity of MR fluids in the channel; τ_{y} is the yield stress of MR fluids which is dependent on the magnetic flux density.

Viscous pressure drop ΔP_{η} is:

$$\Delta P_{\eta} = \frac{6(L+\Delta L)\eta}{\Delta R^2}\dot{x}_{\mathrm{r}} \tag{5}$$

where ΔL is the width of the electromagnetic coil winding; η is the field-off viscosity of MR fluids. Inertial pressure drop is:

$$\Delta P_{\mathrm{I}} = (L + \Delta L)\rho\ddot{x}_{\mathrm{r}} \tag{6}$$

where ρ represents the density of MR fluids; $\ddot{x}_{\mathrm{r}}$ represents the acceleration of MR fluids in the channel.

3. MECHANICAL PERFORMANCE OF THE DEVELOPED MRM-IB

A range of -300 to 300 N loads of the excitation is provided by the test system as shown in Figure 4, and the corresponding excitation velocity is 5 mm/min. Figure 2 shows the force-displacement curves of the developed MRM-IB. The developed MRM-IB provided a quite linear stiffness as seen from the figure. Fitting the force-displacement results of the loading and unloading conditions, the average value of 79 N/mm of the static stiffness is obtained.

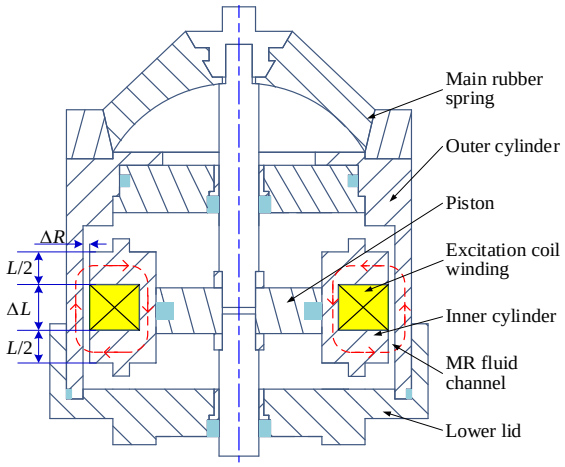

Figure 1. Principle of the proposed MRM-IB.

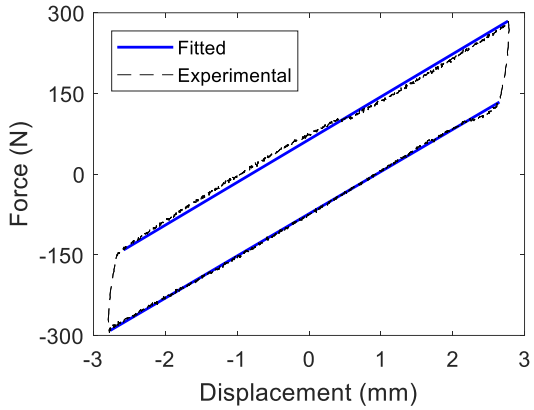

Figure 2. Force-displacement performance of the developed MRM-IB under static loads.

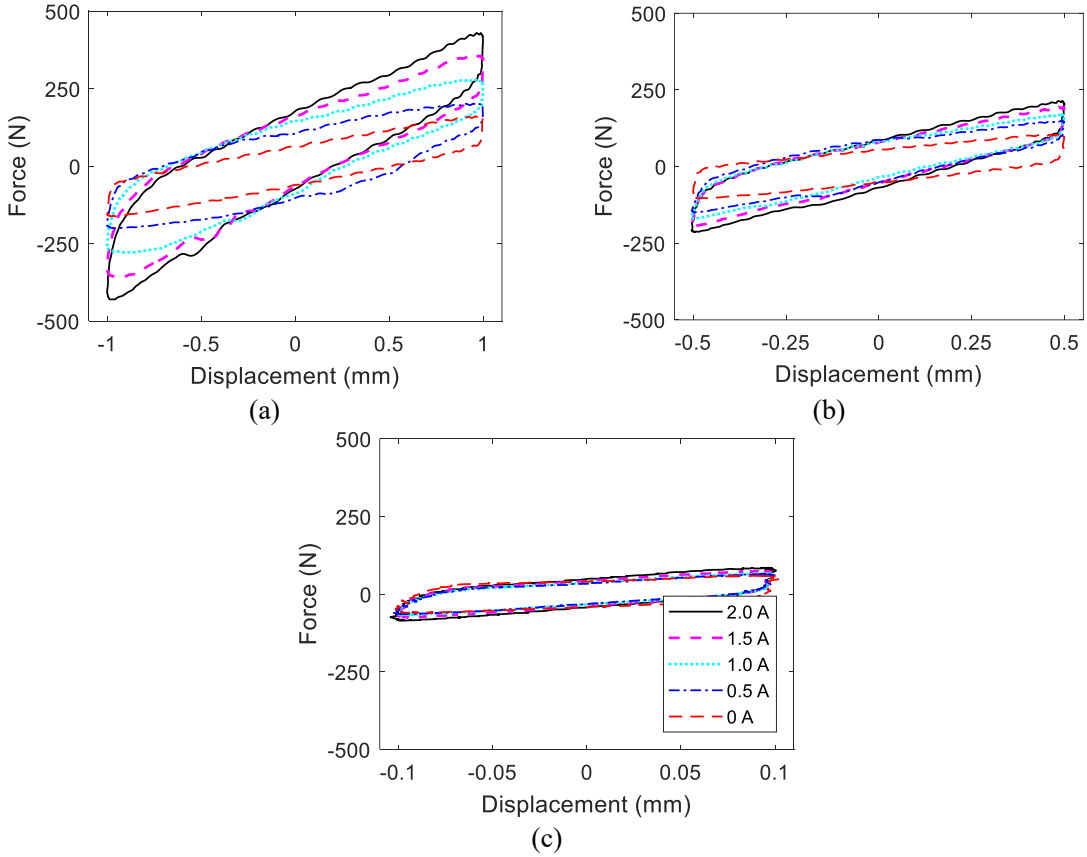

Figure 3. Force-displacement performance of the developed MRM-IB when under 10 Hz sinusoidal displacement excitation with different amplitudes: (a) 1.0 mm, (b) 0.5 mm and (c) 0.1 mm.

Figures 3(a), 3(b) and 3(c) present the force-displacement performance of the MR mount when under 10 Hz sinusoidal displacement excitation. Observing Figure 3(a), when under the excitation with an amplitude of 1 mm, the peak damping force and the area enclosed by the force versus displacement curve both increase with the applied current. Controllable damping property is realized. According to Figures 3(b) and 3(c), when under small displacement excitations, the peak damping force drops due to the MR effect. In order to realize a low field-off dynamic stiffness, the width of the MR fluid channel should be set as large as possible. Therefore, when the excitation amplitude is small and the pressure drops increases with the applied current, the flow magnitude in the MR fluid channel decreases, so that the range of controllable damping force becomes small.

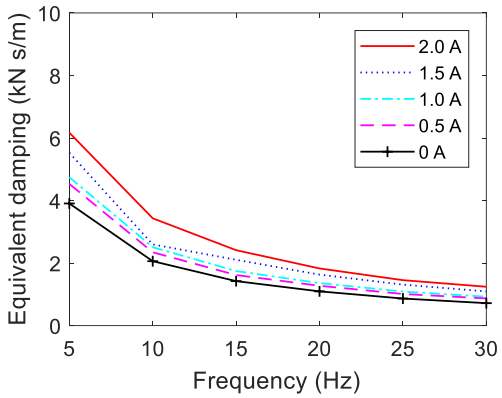

Figure 4. Equivalent damping of the developed MRM-IB under sinusoidal displacement excitation with an amplitude of 0.5 mm.

Figures 4 presents the equivalent damping of the developed MRM-IB varies with the excitation frequency and the applied current when under sinusoidal displacement excitation with an amplitude of 0.5 mm. According to Figure 4, the equivalent damping of the developed MRM-IB nonlinearly increases with the applied current. When over 20 Hz, the effect of the applied current on equivalent damping is weakened. The equivalent damping nonlinearly drops with the increase of the frequency.

4. TESTS OF THE MRM-IB BASED ENGINE SYSTEM WITH FUZZY CONTROLLER

The second-order frequency of engine and the absolute value of acceleration of engine at the mount side are selected as the inputs of the fuzzy controller and the output variable is the applied current. Figure 5 presents the schematic of the fuzzy control system of the MRM-IB with a frequency-identification function based on FFT. Surface of the fuzzy control rules is shown in Figure 6. The applied current shows a relationship with not only the rotational speed but also the vibration acceleration. That is to say, the applied current decreases with the increase of the second-order frequency and rotational speeds.

Table 1 presents the comparison of the root mean square (RMS) values of the acceleration at four rotational speeds corresponding to the state of idle, low, medium and high speed. The vibration acceleration under the fuzzy controller decreases by 22.4%, 9.9%, 3.3%, 0.3%, respectively, which is shown in Table 1. The reasonable performance of the MR mount system on engine vibration isolation at low frequencies is verified again.

Figures 7(a) and 7(b) present the simulated and experimental results of the frequency response of the acceleration. As compared with the passive state, the fuzzy controller significantly reduces the peak of the second-order frequency of the acceleration. As the frequency increases, the control effectiveness gradually decreases. High efficiency of the fuzzy controller is verified by the results of both the experimental tests and simulation in Figure 7.

Figures 8(a) and 8(b) present response of the accelerations in the frequency domain when under startup and shutdown states. It is seen from results that vibration suppression can be realized by the fuzzy controller under any condition. That is to say, the fuzzy controller provides great vibration isolation performance, and the vibration displacement is significantly suppressed.

According to the simulation and experimental tests, the fuzzy controller greatly meets the requirements in vibration isolation of the mount system. When at low frequencies and accelerations, the mount under fuzzy control shows the characteristic of large damping so as to effectively isolate the vibration and reduce the vibration displacement of the engine. When at high frequencies and accelerations, the mount has small damping to attenuate high-frequency noises and reduces the vibration transmitted from the engine to the frame. In other words, the damping of the developed MRM-IB can be improved by increasing the applied current at low frequencies and accelerations. When at high frequencies, the developed MRM-IB keeps in a passive state, whose damping should be as small as possible. Due to the division of the fuzzy sets and the influence of the acceleration, fuzzy controller cannot output a constant current according to the frequency response characteristics of the engine, which causes a limitation to the efficiency of the fuzzy controller.

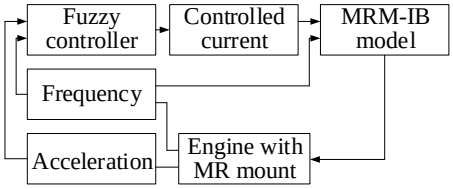

Figure 5. Schematic of the MRM-IB based engine vibration isolation using fuzzy controller.

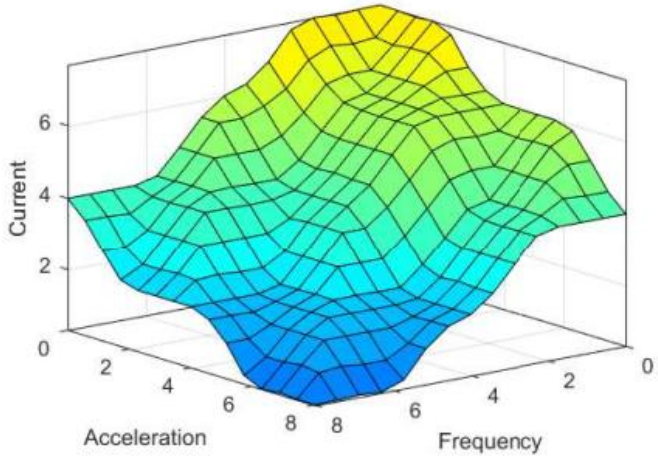

Figure 6. Surface of the fuzzy control rules.

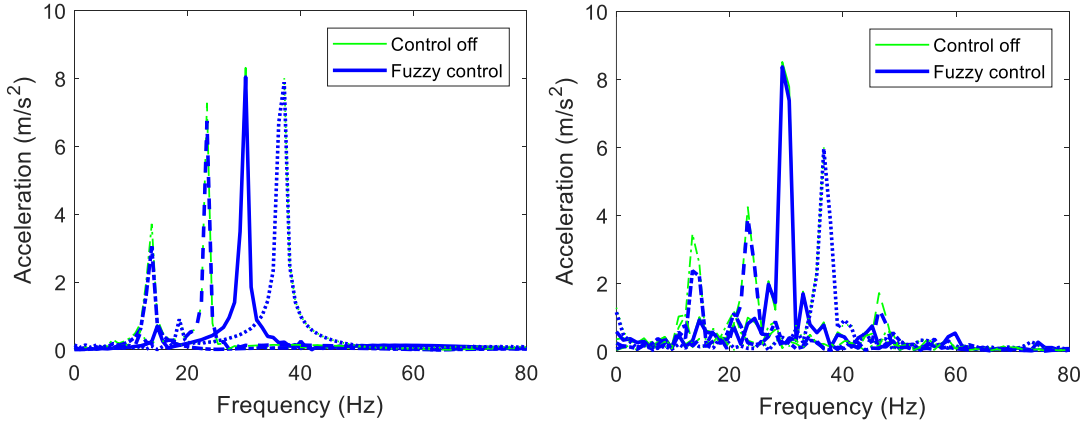

Figure 7. Frequency response of the accelerations when under different rotational speeds: (a) simulated results and (b) experimental results.
Note: Dash-dot line - 800 r/min; Dashed line - 1400 r/min; Solid line - 1800 r/min; and Dotted line - 2200 r/min.

Table 1. RMS value of the acceleration when under different rotational speeds and improvement of the two controllers.

RMS (m/s^2)	Rotational speed (r/min)			
	800	1400	1800	2200
Control off	4.7162	5.5216	11.1772	7.1458
Fuzzy control	3.6583	4.9725	10.8123	7.1241
Improvement percentage	+22.4%	+9.9%	+3.3%	+0.3%

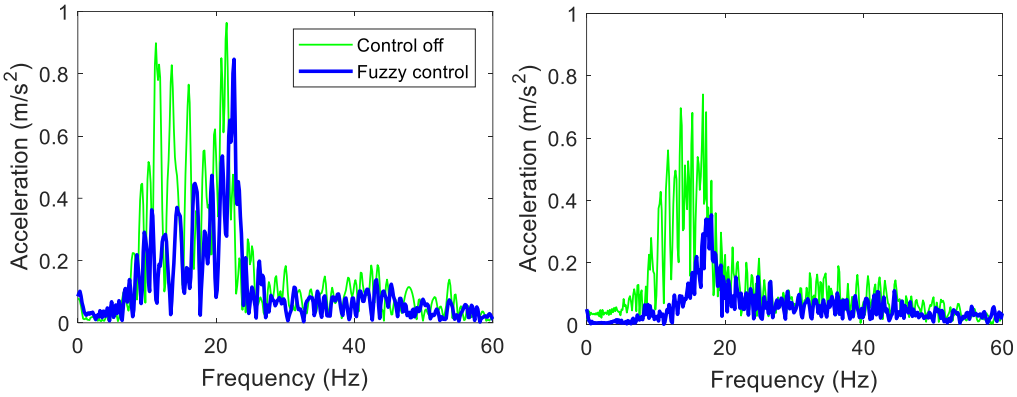

Figure 8. Experimental results of the frequency response of the acceleration when under different conditions: (a) startup and (b) shutdown.

5. CONCLUSION

A MRM-IB with much improved controllable range of dynamic stiffness, field-off dynamic stiffness and working stroke was proposed and investigated in this paper. A fuzzy controller was designed based on the frequency identification. The experimental tests based on the test bench of the engine vibration isolation of the developed MRM-IB was carried out. When the second-order frequency is 13.3 Hz, the RMS values under the fuzzy control decrease by 22.4%. As the frequency increases, the control effect gradually goes weakened. The test results indicate the fuzzy controller is effective in the full frequency range, especially at low frequencies. In addition, as compared with the passive mount system during the start condition, the RMS value of the acceleration under the fuzzy controller decreases by 33.6%, while during the shutdown condition, the RMS value decreases by 55.0%.

ACKNOWLEDGEMENTS

The authors wish to acknowledge the financial support from Tai'an Special Vehicle Co., Ltd (Project No. W2020JSKF0060).

DECLARATION OF CONFLICTING INTERESTS

The authors declared no potential conflicts of interest with respect to the research, authorship, and/or publication of this article.

REFERENCES

[1] Ahamed R, Choi S B and Ferdaus M M, A state of art on magneto-rheological materials and their potential applications, *Journal of Intelligent Material Systems and Structures*, Vol. 29, No. 10, pp. 2051-2095, 2018

[2] Bai X X, Cai F L and Chen P, Resistor-capacitor (RC) operator-based hysteresis model for magnetorheological (MR) dampers, *Mechanical Systems and Signal Processing*, Vol. 117, pp. 157-169, 2019

[3] Nguyen T, Elahinia M and Wang S, Hydraulic hybrid vehicle vibration isolation control with magnetorheological fluid mounts, *International Journal of Vehicle Design*, Vol. 63, No. 2-3, pp. 199-222, 2013

[4] Christie M D, Sun S, Deng L, Ning D H, Du H, Zhang S W and Li W H, A variable resonance magnetorheological-fluid-based pendulum tuned mass damper for seismic vibration suppression, *Mechanical Systems and Signal Processing*, Vol. 116, pp. 530-544, 2019

[5] Cheng H, Wang M, Liu C and Wereley N M, Improving sedimentation stability of magnetorheological fluids using an organic molecular particle coating, *Smart Materials and Structures*, Vol. 27, No. 7, Article No. 075030, 2018

[6] Li Z, Liao C, Fu B, Jian X, Shou M, Zhang H and Xie L, Study of radial flow mode magnetorheological energy absorber with center drain hole, *Smart Materials and Structures*, Vol. 27, No. 10, Article No. 105008, 2018

[7] Phu D X, Shah K and Choi S B, A new magnetorheological mount featured by changeable damping gaps using a

moved-plate valve structure, *Smart Materials and Structures*, Vol. 23, No. 12, Article No. 125022, 2014
[8] Han C, Choi S B, Lee Y S, Kim H T and Kim C H, A new hybrid mount actuator consisting of air spring and magneto-rheological damper for vibration control of a heavy precision stage, *Sensors and Actuators A: Physical*, Vol. 284, pp. 42-51, 2018
[9] Chen P, Bai X X and Qian L J, Magnetorheological fluid behavior in high-frequency oscillatory squeeze mode: experimental tests and modelling, *Journal of Applied Physics*, Vol. 119, No. 10, Article No. 105101, 2016
[10] Chen P, Bai X X, Qian L J and Choi S B, A magneto-rheological fluid mount featuring squeeze mode: analysis and testing, *Smart Materials and Structures*, Vol. 25, No. 5, Article No. 055002, 2016